Journal of Glaciology, Vol. 43, No. 145, 1997

Glacial regime of the highest Tien Shan mountain, Pobeda–Khan Tengry massif

VLADIMIR B. AIZEN,[1] ELENA M. AIZEN,[1] JEFF DOZIER,[1] JOHN M. MELACK,[1]
DAVID D. SEXTON,[2*] VICTOR N. NESTEROV[3]
[1]*Institute for Computational Earth System Science and School of Environmental Science and Management, University of California, Santa Barbara, California 93106, U.S.A.*
[2]*Scott Polar Research Institute, University of Cambridge, Cambridge CB2 1ER, England*
[3]*Pacific Institute of Oceanology, Far-Eastern Branch of the Russian Academy of Science, Radio 7, Vladivostok, Russia*

ABSTRACT. Major processes controlling the existence of a large sub-continental glacier system were identified on the basis of glaciological, meteorological and isotopic analyses using expeditionary and long-term data. Observations were made on the southern Inylchek glacier located in the Pobeda–Khan Tengry massif, the largest sub-continental glacier system on the northern periphery of central Asia. More than 1200 glaciers with a total area of about 4320 km^2 comprise the massif. Melt is for the most part caused by radiation and is most intensive during periods of anticyclonic weather with föhn development. The proportion of solar radiation input in relation to heat balance is more than 90%. Evaporation and condensation are negligible during most times and comprise 7% of heat expenditure. Accumulation was associated with cold cyclonic weather. Four ice-formation zones were identified, the upper boundary of liquid runoff is at 5200 m and the recrystallization zone is above 5900 m. The calculated net glacier mass is negative, -318 kg m^{-2} a^{-1}, and indicates the degradation of modern Pobeda–Khan Tengry glaciers.

INTRODUCTION

Our study concerns the present condition of continental glaciers at mid-latitudes and the evaluation of snow and glacier resources. Although central Asian glaciers have received a good deal of attention (Konovalov, 1979; Krenke, 1982; Academia Sinica, 1986–87; Yang Zhenniang, 1988; Ma Hong and others, 1992), one of the largest, the Pobeda–Khan Tengry glacier system at the northern periphery of central Asia, has not been well explored. Studies of glacier energy and mass balance in remote alpine watersheds require detailed monitoring of the local climate. Snow accumulation and its metamorphism into firn and ice, snow- and ice-melt and runoff are controlled by the magnitude of energy available to drive these processes.

The first of our investigations of remote high-mountain watersheds at mid-latitudes was completed in the northern Tien Shan, the northern periphery of the central Asian mountain system, an area affected by western cyclonic and northern anticyclonic activity (Aizen and others, 1995, 1996b). In 1990–92, we carried out investigations at the southern periphery of the central Asian mountain system in the Himalaya and southeast Tibet, with monsoon climatic conditions (Aizen and Aizen, 1994a, b). This paper summarizes investigations of local temporal and spatial variations of the mass–energy components in the inner sub-continental central Asian high mountains, characterized by a precipitation deficit at low elevations and increasing moisture at high altitudes.

* Deceased.

The Pobeda (Chinese name Tuomuer)–Khan Tengry massif, composed of more than 1200 glaciers with total area about 4320 km^2, is the largest sub-continental glacier system at the northern periphery of central Asia (Fig. 1). The Pobeda–Khan Tengry glaciers are the major source of the main rivers in those regions of internal drainage in central Asia. These affect the great Tarim and Balkhash hydrographic systems, where 45–50% of total runoff is contributed by glaciers (Dolgushin and Osipova, 1980; Xie and others, 1982).

MEASUREMENTS AND DATA COLLECTION

In the summers of 1989, 1990 and 1992, we conducted expeditionary observations on Inylchek glacier located at the center of Pobeda–Khan Tengry massif (Fig. 2). Inylchek glacier covers all glacial zones from 2900 to 7400 m and has two major branches stretching 60.5 km from east to west. The area of the glacier is 794 km^2.

We carried out the field measurements and observations at four points: the active ablation zone (near the Merc-bakher glacial outburst lake) at 3400 m; at 4150 m, close to the firn line; at 5200 m, the upper level of liquid runoff formation; and at 6100 m in the accumulation zone. We used standard Russian hydrometeorological instruments and four automatic mini-meteorological stations built by Grant Instruments (Cambridge) Ltd, England (Table 1). The data loggers of the stations recorded hourly measurements of net total radiation, total incoming radiation, reflected radiation, atmospheric pressure, snow and ice temperature, and discharge from the ablation plots. Measurements were recorded at two levels (0.5 and 2.0 m) above the surface for

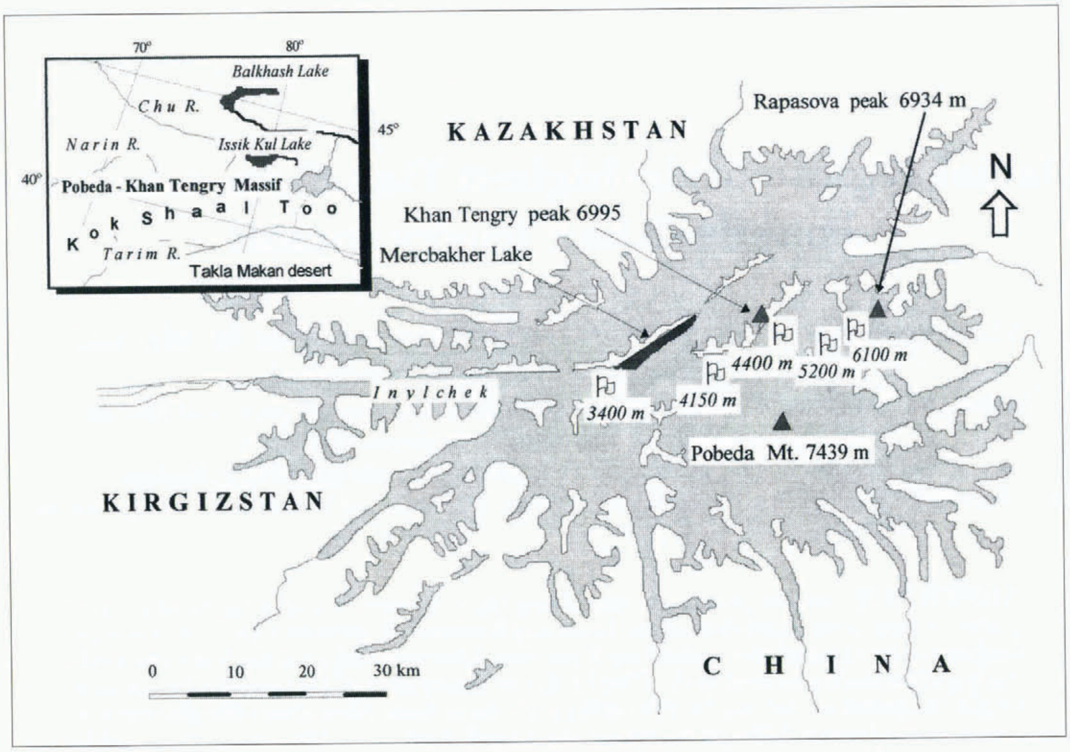

Fig. 1. Pobeda–Khan Tengry glacier massif, central Tien Shan. Shading denotes glaciers; flags are observation stations.

air temperature, relative humidity and wind speed. Wind direction was recorded at 2.0 m. The glaciological observations included measurements of ablation, accumulation and snow–firn–ice stratigraphy in pits and ice cores. Ablation was measured on three slightly inclined 2 × 2 m ablation plots (Fig. 3) at 3500, 4150 and 5200 m. Measurements

Fig. 2. Southern Inylchek glacier.

Table 1. Technical specification of meteorological equipment

X	System	Range	System accuracy
Air temperature	VH-G-Z1 (RAD)	−30 to +70°C	0.4°C
Air humidity	VH-G-Z1 (RAD)	0–100% rh	± 2% rh
Ice temperature	CS-U	−30° to +70°C	0.4°C
Wind direction	W200	< 0.3 to 75 m s^{-1}	>10°
		−25° to +55°C	
Wind speed	A100	−0.15 to 75 m s^{-1}	± 0.1 m s^{-1}
Rainfall, discharge	ARG100	< −30° to +65°C	0.2 mm
Atmospheric pressure	PTB100A	800–1060 mbar	± 0.30 mbar
Solar radiation	SES	300–1100 nm	
	Pyrgeometer	300–4000 nm	
Total radiation	Balansomer	>4000 nm	

were made in the morning and evening at 121 points located within 20 cm cells. Discharge from these plots was measured using a current meter which automatically recorded the passage of water. Snow-density measurements were made in a snow pit located near the ablation squares. The density of melting ice was assumed to be 890 kg m^{-3} (Shumskiy, 1978). The discrepancy between measured ablation and discharge averaged 5 mm.

Measurements of accumulation were made in the accumulation zone at the beginning and end of summer, because maximum precipitation occurs during summer in this region. Depth of snow cover was measured five times at more than 400 points located 50 m from one another. At a single point, the measurement error was on average about 5%. Snow density on the snow surveys was measured by electric balance.

We analyzed the tritium concentration (^{3}H) in atmospheric moisture at 2 m above the surface, in water from glacial channels in different glacial zones (Aizen and others, 1996a) and in samples collected from snow and firn pits and obtained by hand drilling. The collection interval throughout the core varied from 5 to 30 cm depending on the homo-

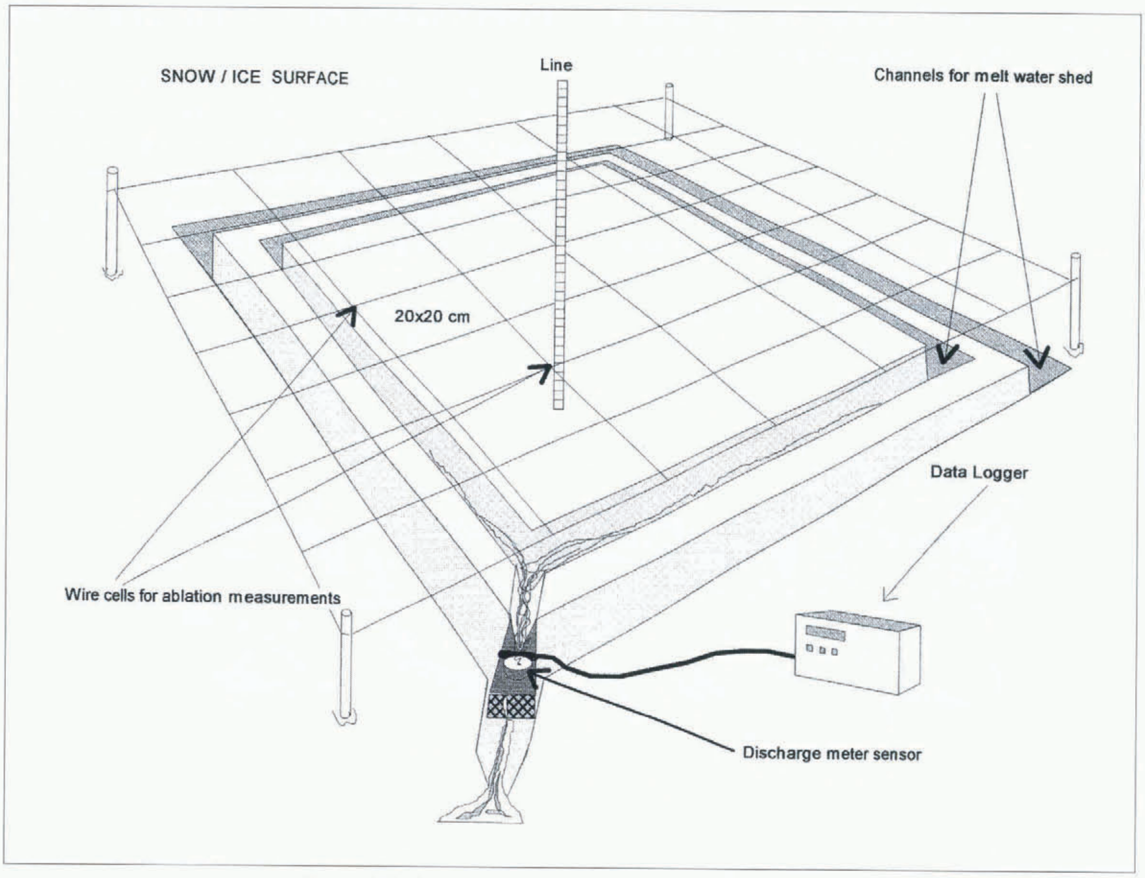

Fig. 3. Ablation plot for measurements of ice- and snowmelt.

geneity of the layers. The equilibration technique for the preparation of samples was applied (Epstein and Mayeda, 1953). The precision of the samples data was 1–10 TU.

The statistical analysis and simulation of present and past meteorological conditions in this region were based on long-term data from a meteorological station located 150 km west of the glacier massif. The station operated from 1930 to 1990 (Kobisheva, 1990). We also used precipitation data collected from 1959 to 1972 at sites located at altitudes from 2800 to 4200 m in the Inylchek glacier basin. Topographic maps of the central Tien Shan region at 1:25 000 scale and synoptic maps of surface and 500 mbar were also used.

METHODS OF CALCULATION OF HEAT AND MASS BALANCE

The simplified thermal balance equation may be stated as:

$$lW = B + P_{\mathrm{t}} \pm \mathrm{LE} \tag{1}$$

where W is the melt intensity at a point (kg m^{-2}); l is the latent heat of ice fusion (J kg^{-1}); B is the total radiation balance (J m^{-2}), including the shortwave radiation balance ($Q(1-A)$) and longwave radiation balance; Q is the incoming shortwave radiation; A is the surface albedo; P_{t} is the turbulent-heat flux from the atmosphere (J m^{-2}); LE is the latent-heat flux due to evaporation or condensation (J m^{-2}). Using hourly gradient measurements, turbulent heat and humidity fluxes were calculated from functions of similarity computed using Equation (2). All calculations were carried out using the theory of the surface boundary layer in a homogeneous fluid, developed by Monin and Obukhov (1954) and Kazanskiy (1965).

$$d > 0: \quad f_t(x) = f_q(x) = 1 + 5x \tag{2}$$

$$d < 0: \quad f_t(x) = (1 - 16x)^{1/2}; \quad f_v(x) = (1 - 16x)^{1/2}$$
$$x = (z - d_{\mathrm{o}})/d \tag{3}$$

where t (°C) is the air temperature, q (mbar) is air humidity, v (m s^{-1}) is wind, d is the distance found from non-linear equations, d_{o} is surface roughness, z is height of measurements above the surface. Evaporation was also measured by repeated weighing of decimeter cubes of snow and firn using an electric balance with an accuracy of 0.1 g.

To calculate an annual mass-balance index (I_{bi}), Equation (4) was used. All components were determined at the long-term mean altitude of the equilibrium-line position ($H_{\mathrm{e.l.}} = 4476$ m) which was calculated using Kurowski's (1891) method. We assume this elevation is the level of the average characteristics of mass exchange (Ahlmann, 1940; Krenke, 1982).

$$I_{\mathrm{bi}} = P_{\mathrm{e.l.}} - W_{\mathrm{e.l.}} \pm E_{\mathrm{e.l.}} + J_{\mathrm{e.l.}} \tag{4}$$

where $P_{\mathrm{e.l.}}$ is annual solid precipitation (from October to September) at the altitude of the equilibrium-line position, $W_{\mathrm{e.l.}}$ is total glacier melt, $E_{\mathrm{e.l.}}$ is the mass of evaporation or condensation and $J_{\mathrm{e.l.}}$ is refrozen meltwater.

The total precipitation was calculated as

$$P_{\mathrm{e.l.}} = P_0 + \gamma(P)(H_{\mathrm{e.l.}} - H_0) \tag{5}$$

where P_0 (mm) is mean precipitation at the Tien Shan meteorological station at $H_0 = 3614$ m a.s.l.; $\gamma(P)$, (0.52 mm/m) is mean altitudinal gradient of precipitation calculated from data at the Tien Shan meteorological station (308 mm) and long-term data from precipitation sites at 4200 m (673 mm).

To estimate the total glacier melt, the air temperature at the altitude of the equilibrium-line position was calculated as

$$T_{\mathrm{e.l.}} = T_0 - \gamma(t)(H_{\mathrm{e.l.}} - H_0) \qquad (6)$$

where T_0 (°C) is mean air temperature at the Tien Shan meteorological station; $\gamma(T)$ ($0.0053\,°\mathrm{C\,m^{-1}}$) is mean altitudinal gradient of air temperature calculated from data at the Tien Shan meteorological station and expeditionary observations at 4150 m on the glacier.

CIRCULATION AND CLIMATIC PROCESSES

The high ranges surrounding central Tien Shan prevent the entrance of moisture; hence, winter precipitation is small, especially in January and February, accounting for only 8–10% of the total in this region (Kobisheva, 1990). In summer, the level of condensation rises, which leads to a precipitation increase at high elevations. Development of convection and strengthening of unstable atmospheric stratification result in a summer maximum of precipitation in June and July caused by cold moist air masses from the west. At the same time, these high mountains are an obstacle to dry tropical

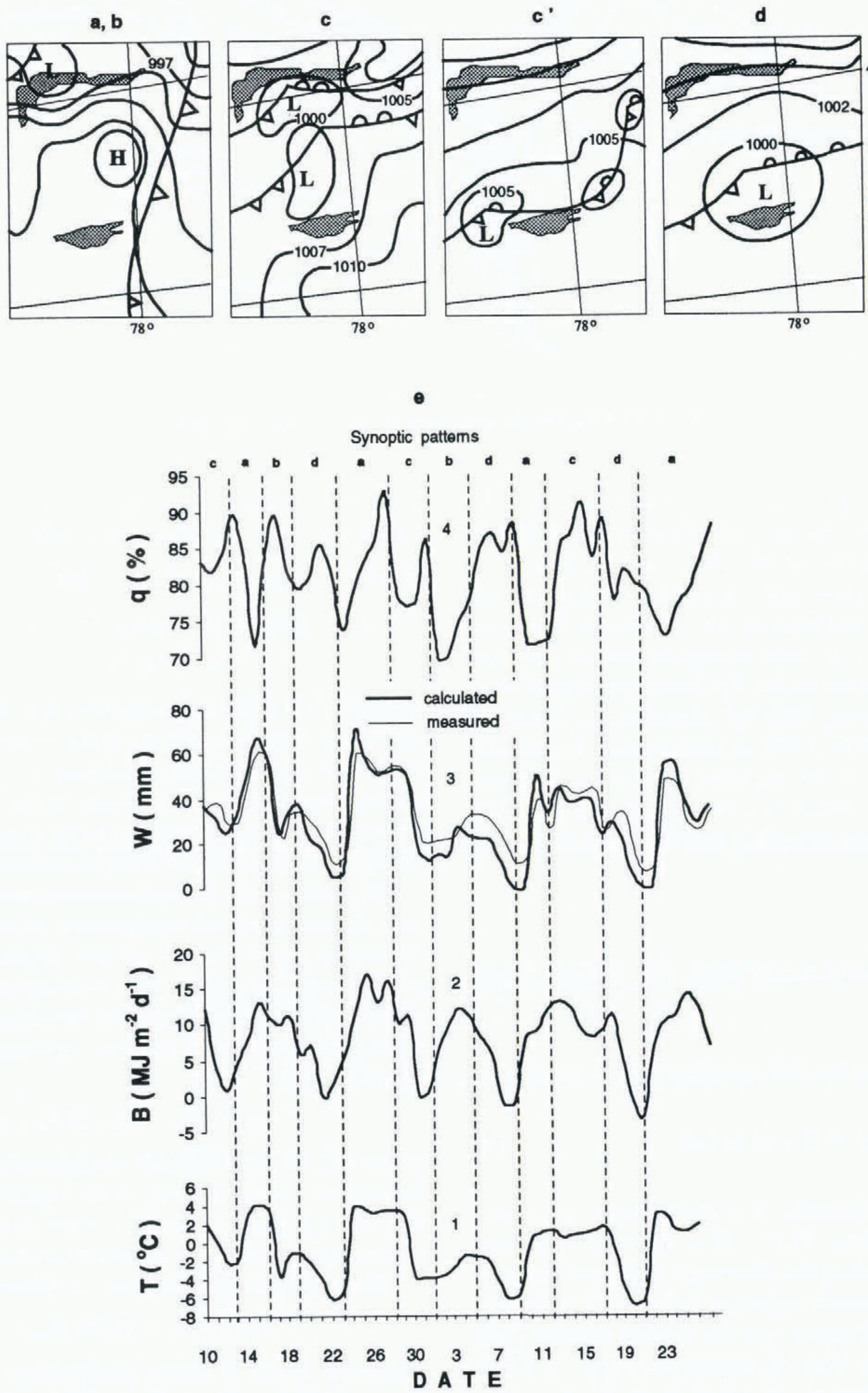

Fig. 4. Synoptic (a–d) and meteorological (e) conditions at 4150 m on southern Inylchek glacier during the ablation period (July–August 1989) of the expeditionary observations. (a) and (b) are anticyclonic warm and cold weather; (c) and (c') are cyclonic warm weather; (d) is cyclonic cold weather; (e) is diurnal mean air temperature (1); total radiation balance (2); glacier ablation (3); relative humidity (4).

air masses formed over the Takla Makan, Gobi, Alashan and Tsaidam deserts and moved to the north. These processes have a substantial effect on the mass and energy exchange of the glaciers.

According to our observations on Inylchek glacier and the analyses of synoptic maps, there are four main synoptic processes (Fig. 4; Table 2):

Anticyclonic weather with föhn development (A_w) is the most favorable synoptic process for glacier ablation, observed with 33% frequency during two expeditionary summers. Dry föhns with low relative humidity occurred after an advection of cold air masses. Warm air masses over the Takla Makan desert flow up the southern slopes of the Kok Shaal Too range and pass down into the Inylchek glacier and other adjoining valleys. A föhn cloudiness is formed above the ridge-top, while air temperature can rapidly increase by 5°C on the glacier. A large amount of loess dust is brought into the valley with föhn winds. The atmosphere becomes less transparent and longwave radiation increases. In two summers, the total radiation balance reached its maximum of 15 MJ m^{-2} d^{-1} and albedo its minimum (34%) (Table 2). Glacier melt intensified abruptly because of heat advection. Turbulent-heat exchange in heat balance was 6% (Table 2), whereas during the other observed types of weather the turbulent component did not play a significant role in glacier melt. This period was characterized by the contribution of condensation heat to the heat balance. Despite the föhn advection, humidity remained relatively high (76%). High humidity and aerosol dust cause the formation of inter-mass cloudiness and local precipitation, especially at elevations above 5000 m. According to Berg (1938) and Grudzinskiy (1959), aerosol dust is delivered from northwest of Kazakhstan and Turan to the central Tien Shan. However, our observations indicated that dust is delivered by air fluxes from central Asian deserts. During this synoptic process, melt was maximum, did not stop even at night and averaged 47 mm d^{-1}. During föhn development, it reached 82 mm d^{-1}.

Anticyclonic cold weather (A_c) without precipitation occurs as cold-air intrusions and is followed by a slight temperature increase due to insolation and a transition to thermal depression. The frequency of this type was 19%. There was a slight decrease in net shortwave radiation and total radiation balance compared to anticyclonic warm weather (Table 2). Melt associated with radiation amounted to 23 mm d^{-1}. Due to high values of radiation balance, ice- and snowmelt took place at negative air temperatures with a diurnal mean of −3.3°C. During this weather, latent heat and turbulent exchange did not play any significant role in heat balance and refreezing occurred. Relative humidity rose to 86%.

Cyclonic warm weather (C_w) occurred with a frequency of 24%. The regime is associated with northwestern intrusions, when the cold front lingering near the mountains develops wave activity (Fig. 4b and c) and brings inclement weather with frequent mixed precipitation. During such periods, rain was observed even at 4150 m. Net shortwave radiation falls to 19.2 MJ m^{-2} d^{-1}, albedo reaches 48%, while total radiation balance falls to 5.6 MJ m^{-2} d^{-1}. Mean diurnal temperature was 0.9°C. Evaporation in such periods prevails over condensation, reaching 13%. Melt amounted to 15 mm d^{-1}.

Cyclonic cold weather (C_c) had 24% frequency. Cyclonic activity develops in mid-latitudes of central Asia. Cold intrusions bring precipitation (Fig. 4d). During this weather in summer, snowfall plays a key role in glacier accumulation. Net shortwave radiation (20.1 MJ m^{-2} d^{-1}) was higher than during warm cyclonic processes, because of multiple reflection from slopes covered by new snow. Albedo increased to 70%. In such periods, we observed the lowest values of temperature (−6.9°C) and total radiation balance (2.6 MJ m^{-2} d^{-1}). Ice- and snowmelt averaged 7 mm d^{-1} from radiation alone with little turbulent exchange (only 2%).

RESULTS OF EXPEDITIONARY MEASUREMENTS

Heat-balance component

During summer expeditionary observations in 1989 and 1990 at 4150 m, incoming radiation amounted to 96% of the heat-balance total, while turbulent heat was about 4% of the total. Heats of evaporation and condensation at 4150 m were negligible (Table 2) and, on the whole, were compensatory, taking only 7% of heat for evaporation. Evaporation prevails on average in daytime, and condensation at night, with the exception of föhn days when condensation operates continuously (day and night). The major part of incoming radiation is used for ice- and snowmelt.

Snow- and icemelt occur through radiation (Table 2)

Table 2. Average components of the heat balance and mean meteorological characteristics during different synoptic processes (SP) of ablation period (June–August, 1989, 1990) at 4150 m of Inylchek glacier. A_w and A_c are anticyclonic warm and cold weather; C_w and C_c are cyclonic warm and cold weather; Q is net shortwave radiation; B is total radiation balance; P_t is turbulent-heat fluxes; LE is latent-heat fluxes due to evaporation or condensation; lW is heat used for ice- and snowmelt; A is albedo; q is relative humidity; f is frequency of synoptic process; T is air temperature

SP	*Q*	*B*	P_t	*LE*	*lW*	*B*	P_t	*lW*	*LE*	*A*	*q*	*f*	*T*
			MJ m^{-2} d^{-1}				Proportion in heat balance			%	%	%	%°C
A_w	30.5	14.9	0.9	0	−15.8	94	6	100	0	34	76	33	3.1
Ac	26.9	8.9	0.1	−1.2	−7.8	98	2	87	13	51	86	19	−3.3
Cw	19.2	5.6	0.4	−0.8	−5.2	93	7	87	13	48	87	24	0.9
Cc	20.1	2.6	0.05	−0.2	−2.45	98	2	93	7	70	89	24	−6.9
Whole	24.6	8.5	0.4	−0.5	−8.5	96	4	93	7	49			

and can proceed with both positive and negative air temperatures. Snow- and icemelt were calculated three ways: through heat balance (Equation (1)), solar radiation data (Equation (7)) and air temperature associated with different air-flow patterns (Equations (8)–(9)). Equations (7)–(9) were based on expeditionary measurements made on Inylchek glacier and were checked on the other glaciers of the Pobeda–Khan Tengry massif.

$$W_\mathrm{d} = 1.59 \times 10^{-3}[23.9Q(1 - A/100)]^{1.68} \quad r = 0.73 \quad (7)$$

where W_d is the daily value of snow, ice and firn melt ($\mathrm{mm\,d^{-1}}$), Q is the daily net shortwave radiation during summer ($\mathrm{MJ\,m^{-2}\,d^{-1}}$), A is the albedo (%).

$$W_\mathrm{d}(A_\mathrm{w}, C_\mathrm{w}) = 12.1 + 12.5T \quad \text{when } T > 0.9^\circ\mathrm{C} \quad r = 0.71 \quad (8)$$

$$W_\mathrm{d}(A_\mathrm{c}, C_\mathrm{c}) = 40.0 + 4.6T \quad \text{when } T < 0.9^\circ \quad (9)$$

where $W_\mathrm{d}(A_\mathrm{w}, C_\mathrm{w})$ is melt during warm anticyclonic (A_w) and cyclonic (C_w) weather patterns ($\mathrm{mm\,d^{-1}}$), $W_\mathrm{d}(A_\mathrm{c}, C_\mathrm{c})$ is the melt during cold patterns ($A_\mathrm{c}, C_\mathrm{c}$) of weather ($\mathrm{mm\,d^{-1}}$).

Means of daily melt calculated by these methods were close (Table 3). The relative error between calculated and measured values of melt was 2.3–7.6% of the average. Therefore, it is possible to calculate the melt through the solar radiation data (Equation (7)) or to use air temperature associated with different air-flow patterns (Equations (8)–(9)).

Intensity of melt on Inylchek glacier was high and reached 12.5 mm and 1°C.

Meteorological regime

The average diurnal air temperatures, their variation between glacial and non-glacial surfaces, and radiation balance and relative humidity during different types of weather observed during two summer expeditions are presented in Figure 5a–e.

Maximum diurnal variation of radiation balance was observed during anticyclonic types of weather, while the highest diurnal amplitudes of air temperature occurred during cold types of weather with substantial cooling at night and heating during daytime. The altitudinal gradient of air temperature calculated based on observational data at altitudes of 3200, 4150, 5100 and 6100 m was found to be, on average, 0.36°C per 100 m over a glacial surface. A statistically significant correlation ($r = 0.84$) was revealed between mean daily air temperatures at the Tien Shan meteorological station and at 4150 m, on Inylchek glacier. The altitudinal gradient of the air temperature based on records at the Tien Shan meteorological station and at 4150 m on the glacier amounted to –0.53°C per 100 m.

Anticyclonic weather was characterized by the highest frequency of northern and eastern winds (81%), especially in the first half-day. Mean wind speed in anticyclonic weather did not exceed 1.2 m s^{-1}, since calms were rather frequent at that time. During cyclonic processes, the frequency of

Table 3. Calculated means of ice- and snowmelt (W mm d^{-1}) and measured ablation (A_m mm d^{-1}) during different synoptic processes (SP) of ablation period (June–August 1989, 1990) at 4150 m of Inylchek glacier. A_w and A_c are anticyclonic warm and cold weather; C_w and C_c are cyclonic warm and cold weather; $W_\mathrm{h.b.}$ is calculated melt though heat balance; $W(T)$ is calculated melt though air temperature; $W(Q)$ is calculated melt though shortwave radiation balance

SP	$W_\mathrm{h.b.}$	$W(T)$	$W(Q)$	A_m
A_w	−47	−1	−51	−44
A_c	−23	−25	−25	−22
C_w	−15	−23	−16	−19
C_c	−7	−8	−7	−1
Whole	−25	−29	−27	−23

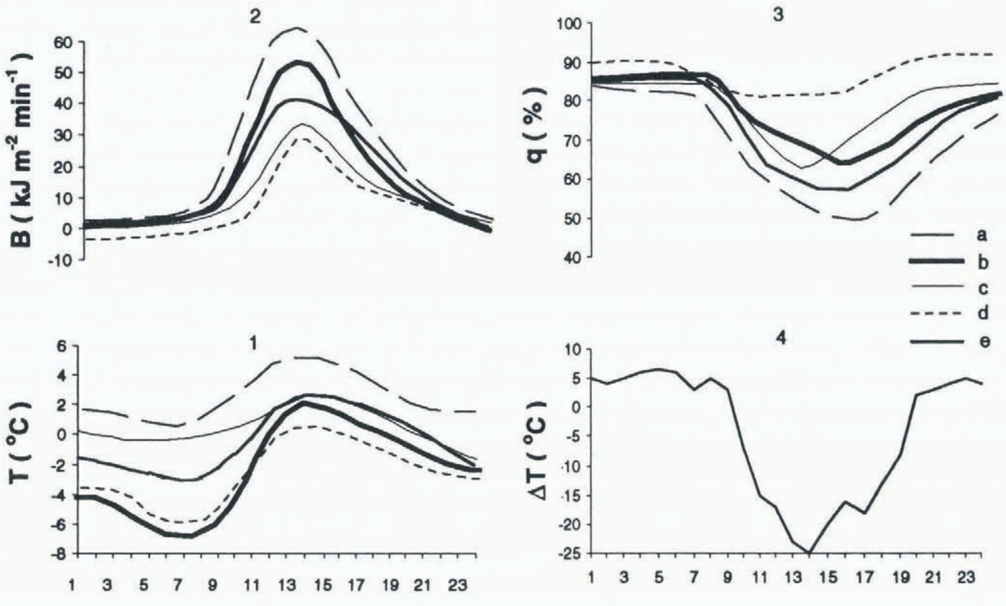

Fig. 5. Diurnal variation of mean meteorological characteristics during different synoptic patterns at 4150 m on southern Inylchek glacier during the ablation period (July–August 1989) of expeditionary observations. (1) is air temperature; (2) is total radiation balance; (3) is relative humidity; (4) is air-temperature difference between glacier and moraine. (a) is anticyclonic warm; (b) is anticyclonic cold; (c) is cyclonic warm; (d) is cyclonic cold weather; (e) is average during whole expeditionary period.

western and northern winds increased to 75% and their speed reached 2.7 m s^{-1}.

Tritium measurements

At 4150 m, the concentration of tritium in atmospheric moisture varies from 59 to 154 TU over the observation period (Table 4; Fig. 6). At 5200 m, the concentration of tritium in atmospheric moisture varies from 610 to 1277 TU. The high concentration of tritium there might be associated with a penetration of stratospheric moisture through a rupture of the tropopause during the passage of atmospheric jet streams, or with other natural phenomena, including heliophysical ones. Using tritium analysis (^{3}H), we obtained the pattern of diurnal runoff distribution in water courses in the ablation zone. The abrupt increase in tritium concentration in ice meltwater at night in the ablation area results from runoff from the warm firn zone. This assumption is supported by the increased tritium content at night observed only in watercourses that have direct connections with the accumulation area. In smaller watercourses, especially in those lying close to moraines, night-time tritium concentrations are similar to the daytime values.

STUDIES IN THE ACCUMULATION AREA

The firn fields of southern Inylchek glacier stretch from southeast to northwest, from the slopes of the Voyennikh Topografov (6873 m) and Rapasov's (6934 m) peaks to the base of Khan–Tengry peak. The area is more than 30 km^2 and the difference between the lowest and highest points is 1900 m (Fig. 7). A 700 m high icefall divides this area into

Table 4. Range of tritium concentration (^{3}H, TU) in samples of atmospheric moisture (am), glacier runoff (gr), channel water (cw), water in glacial lakes (wl), new snow (ns), surface snow (ss), moister firn (mf) and ice (i) in Inylchek glacier in July and August, 1989

H (m)	*am*	*gr*	*cw*	*wl*	*ns*	*ss*	*mf*	*i*
1200		48	6–20					
4100	59–154			4	50–53	52–61		3–4
5100	610–1277			38	39–45		40	54

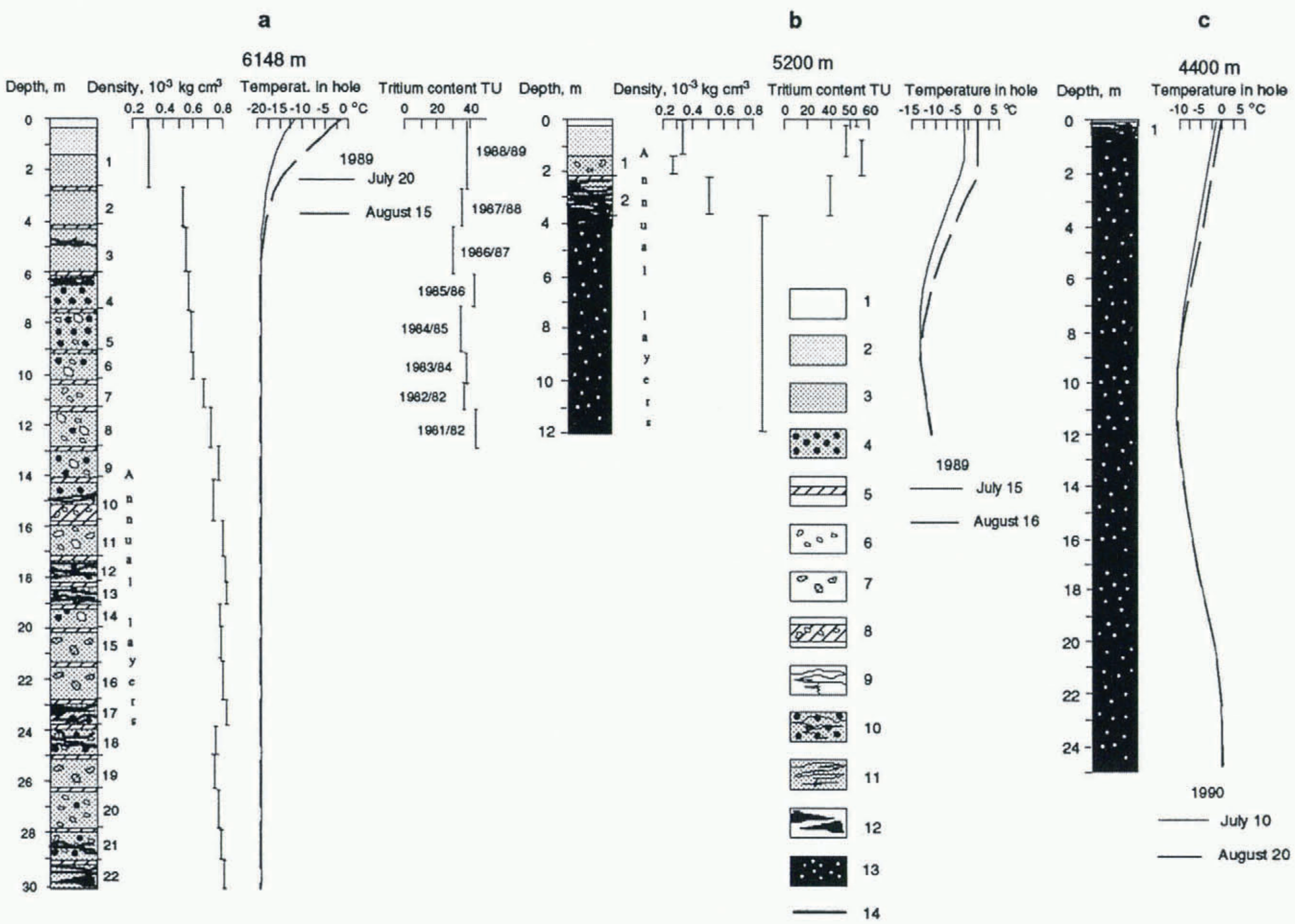

Fig. 6. Stratigraphic profiles of snow, firn and ice; the temperature in drillholes and tritium content in samples from the snow, firn and ice cores at 6148 m (a), 5200 m (b), 4400 m (c) of southern Inylchek glacier. (1) is new snow, (2) is fine-grained firn, (3) is medium-grained firn, (4) is coarse-grained firn, (5) is crust with dust, (6) is ice lens, (7) is dense-firn lens, (8) is crust dust and ice lens, (9) is trace of get-wet-through firn layer, (10) is get-wet layer coarse-grained firn, (11) is get-wet layer medium-grained firn, (12) is ice crust, (13) is monolith of ice, (14) is marks of annual layers.

https://doi.org/10.3189/S0022143000035115 Published online by Cambridge University Press

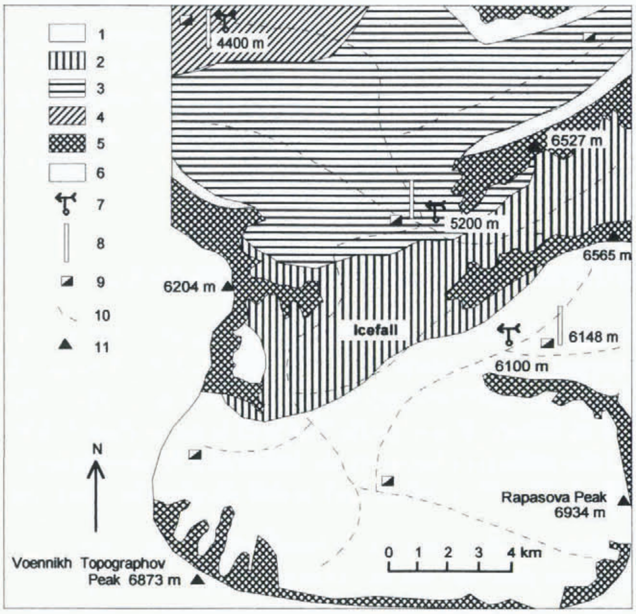

Fig. 7. Ice-formation zones on firn field of southern Inylchek glacier. (1) is recrystallization, (2) is recrystallization–regelation and cold infiltration, (3) is warm infiltration, (4) is infiltration, (5) is rocks, (6) is moraine terrace, (7) is observation site, (8) is drilling holes, (9) is snow pits, (10) is snow-survey transects, (11) is altimetric points.

two main parts with slightly inclined surfaces, one from 4400 to 5200 m and the other from 5800 to 6300 m. The minimal wind and absence of snow-avalanche redistribution inside this area are favorable for the natural accumulation of precipitation. The steady snow regime is proved by its small spatial variability ($\sigma = \pm 88\,\mathrm{kg\,m^{-2}}$).

According to our observations in 1989, 1990 and 1992, snowmelt and runoff in the accumulation area occurred to 5200 m, whereas on southern slopes this boundary reached 5800 m. The annual accumulation here is saturated and, during the day, air temperatures are about zero. During anticyclonic weather, a thin radiation ice crust is formed on the snow surface. Under the crusts, meltwater forms vast "firn bogs" in places with slight inclinations and depressions. Night cooling is insufficient to freeze this moist snowpack, therefore meltwater was drained from this zone during day and night.

From 5800 to 6300 m, the annual mean snow accumulation was found to be 918 g m^{-2} (in 1989). Simultaneous measurements of precipitation, occurring during the observational periods at 5200 and 6100 m revealed an altitudinal increase of precipitation of 2 mm per 100 m.

To assess the annual accumulation and temperature, two cores about 30 m long were drilled at 6148 m. Figure 6 shows the structure of two averaged snow–firn cores. Twenty-one annual layers of accumulation were separated in the drilled holes by snow–firn–ice-core stratigraphic analysis and 23 in the 28 m depth section along the cleared firn–ice wall of the crevasse at the same altitude. Annual layers were identified by summer horizons of more compact firn and yellow-brown aeolian dust. According to our and previous studies (Racek, 1954), dust indicating the annual layers is delivered from deserts only in the second half of summer and beginning of autumn during steady anticyclonical weather.

Verification of annual layers was also made by tritium (^{3}H) sampled from the strata (Fig. 6). The marks were the layers accumulated during rather high tritium content in 1981–82 and 1985–86, caused by nuclear tests conducted in China and the disaster at Chernobyl. According to identification of the annual layers in the cores, the mean annual snow accumulation was found to be 900 mm (Table 5) at 6148 m. Results of stratigraphic analyses are justified by a good correlation (Equation (10)) between annual accumulation measured at 6148 m and annual precipitation measured at Tien Shan station.

$$A_\mathrm{k} = 27.7P^{0.61}\,, \qquad (r = 0.89) \tag{10}$$

where A_k is accumulation over the hydrological year (from September to August) in Inylchek glacier (6148 m), P is annual precipitation measured at Tien Shan station, and η is the correlation ratio. According to Chinese results (Cheng Tong, 1982), the annual precipitation was about 800 mm at the same altitudes on the southern slope of Kok Shaal Too near Pobeda peak. Increase of precipitation with altitude is not a linear function (Fig. 8). The altitudinal distribution of precipitation was calculated on the basis of long-term meteorological data from the Tien Shan meteorological station, precipitation sites and snow surveys in the Inylchek glacier area.

Four ice-formation zones have been revealed in the southern Inylchek accumulation area (Fig. 7), none of them having any clearly delineated distribution area. The icefall dividing the accumulation area into two parts seems to lie in the cold infiltration–recrystallization zone where the meltwater becomes ice due to infiltration. Stratification analysis of snow–firn layers has shown that above 6000 m ice was formed by subsidence and recrystallization at depth exceeding 30 m. Therefore, the altitudinal belt over 6000 m we determined as a recrystallization zone where melt does not occur.

Table 5. Thickness of annual snow–firn layers (h_i, cm), density (ρ_i, Mg m^{-3}) and water equivalent (C_i, mm) in the recrystallization zone of Inylchek glacier, 14–15 August 1989, at 6148 m

Year	h_i	ρ_i	C_i
1989	275	0.32	880
1988	152	0.53	806
1987	170	0.55	935
1986	160	0.57	912
1985	146	0.58	847
1984	114	0.6	684
1983	105	0.68	714
1982	138	0.71	980
1981	130	0.78	1014
1980	137	0.73	1000
1979	133	0.8	1064
1978	97	0.81	786
1977	88	0.83	730
1976	97	0.78	757
1975	123	0.79	972
1974	137	0.8	1096
1973	90	0.83	747
1972	124	0.76	942
1971	129	0.74	955
1970	135	0.77	1039
1969	133	0.79	1051
Average			900

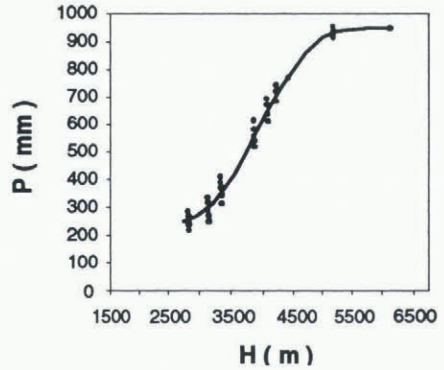

Fig. 8. Vertical change of annual precipitation in Inylchek valley.

The value of ice formation in lower zones (F) was calculated by Zikin's method (Zikin, 1962).

$$F = \frac{cp}{l} \int_{Z_1}^{z} \Delta T(Z)\, \mathrm{d}z\,, \tag{11}$$

where $c = 2.09 \times 10^3\,\mathrm{J\,kg^{-1}\,°C^{-1}}$ is specific heat capacity of ice; $l = 333.6 \times 10^3\,\mathrm{J\,kg^{-1}}$ is heat of ice melt; p (kg m^{-3}) is ice density; Z_1 (m) is the boundary between firn and ice; Z (m) is the lower boundary of the active ice layer; and ΔT (°C) is ice-temperature variation. Ice temperatures in drillholes at altitudes of 6148, 5200 and 4400 m were measured at the beginning and the end of the ablation period (Fig. 6a and c). The value of ice formation in the warm infiltration–recrystallization zone (4600–5200 m) calculated by Equation (11) was 140 kg m^{-2}, under $p = 880$ kg m^{-3} and $Z = 7$ m. In the infiltration zone (4200–4600 m), the value of ice formation was 90 kg m^{-2}, under $p = 890$ kg m^{-3} and $Z = 9$ m.

In the 30 m hole drilled at 6148 m, diurnal temperature changes were observed only in the top layer of annual accumulation (Fig. 6a). At greater depths, the temperatures were constant and at the bottom the temperature was −21°C, that is, about annual mean air temperature at this elevation. Calculations of mean annual air temperature at this level were made through the Tien Shan station data using the temperature gradient of −0.53°C per 100 m. At 6100 m, in August 1989 and 1990 the mean diurnal air temperature was about −10°C. During daytime, it did not rise over −2.0°C, while at nights it could be as low as −25.0°C. At these altitudes, air temperature and moisture variations depended mostly on the inter-mass processes. Heat flux brought by föhns was not significant there. High humidity, observed especially at night (85–95%), was favorable for hoar-frost formation. The condensation overnight can be as high as 1.5–2.0 mm. At the accumulation area of southern Inylchek glacier screened from the west, the average wind speed was 1.7 m s^{-1}, and never exceeded 6 m s^{-1}. At the same time, on Kok Shaal Too and Tengry Tag slopes, the wind speed reached 40–80 m s^{-1} during cyclonic and föhn weather.

During cloudless weather, at 55–60% relative humidity, the evaporation was 1.5–2.0 mm d^{-1}. It is less than at the same altitudes of western Kun Lun, in an extra-continental climate where evaporation reached 5.5–9.7 mm d^{-1}, with 30% relative humidity (Higuchi and Xie Zichu, 1989). During anticyclonic weather, local vertical fluxes develop cloudiness, humidity increased abruptly and from 1400 to 1500 h snow started. Precipitation from such cloudiness being typically local amounted to 5–7 mm d^{-1}. At nights, the cloudiness was dispersed or disappeared.

MASS BALANCE OF INYLCHEK GLACIER

To calculate annual mass-balance indices of Inylchek glacier (Fig. 9), the long-term data of total precipitation and mean summer air temperatures at the Tien Shan meteorological station were extrapolated up to the elevation of the equilibrium-line position (4476 m). Annual precipitation was calculated by Equation (5), annual ablation by Equations (6), (8) and (9). Assessment of annual melt ($W_{\mathrm{e.l.}}$) has been calculated by

$$W_{\mathrm{e.l.}} = W_{\mathrm{d}} m \tag{12}$$

where m is number of days when melt occurs under the certain state of Equations (8) and (9). We assumed loss by evaporation was compensated by condensation and a consistent value of refrozen meltwater equaled 90 mm a^{-1}. There are cycles of positive and negative deviations in glacier mass-balance indices (Fig. 9). From 1940 to 1953 and from 1973 to the present, the glacier had a negative mass balance. For Inylchek glacier, the average weighted mean annual accumulation is 752 mm, the snow–ice ablation average weighted mean is 1070 mm and the index of net glacier-mass change is negative, −318 kg m^{-2} a^{-1}, indicating degradation of modern Pobeda–Khan Tengry glaciers.

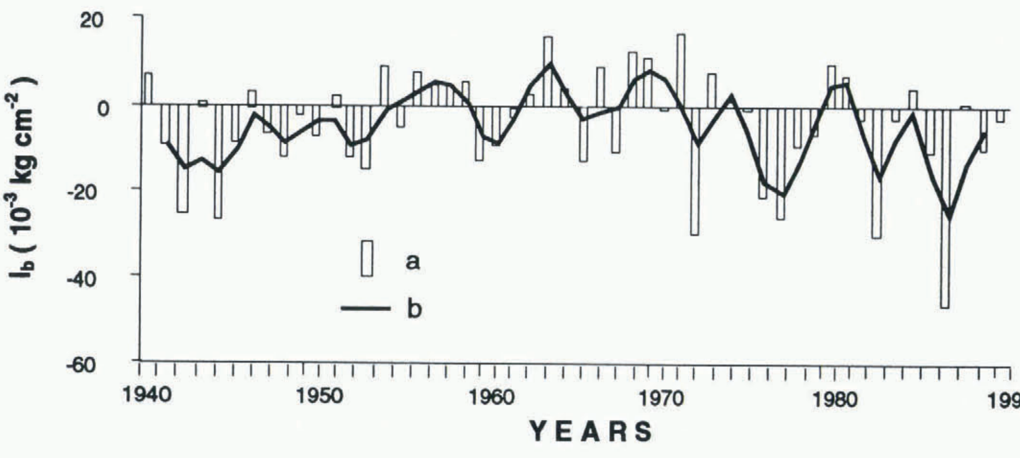

Fig. 9. Indices of glacier mass balance (a) and their centrally weighted moving-average values (b) of Inylchek glacier, central Tien Shan.

https://doi.org/10.3189/S0022143000035115 Published online by Cambridge University Press

CONCLUSIONS

Our analysis extends understanding of the climatic, meteorological and hydroglaciological conditions around the continental glacial Pobeda–Khan Tengry massif, one of the largest in the world.

Four major synoptic situations have been identified, with an average 4 day duration, which control regimes of temperature, radiation balance and melt. In the accumulation area, weather conditions have a smaller effect and a considerable role is determined by internal processes affecting a local water exchange. The development of internal processes is promoted by the high moisture content of air masses coming mostly from the west. At the same time, our observations indicated that dust is delivered by air fluxes from central Asian deserts during the development of föhn.

Radiation contributes more energy for snow and glacier melt than the combination of all other forms of heat transfer and amounts to more than 90% of the input in heat. Melt is most intensive during periods of anticyclonic weather with föhn development. Only at these periods did turbulent exchange and condensation occur. Föhns bringing large amounts of dust from Tarim affect the radiation balance and cause the development of local cloudiness and the formation of precipitation. Because the melt regime is determined there mainly by solar radiation, it was preferable to calculate the melt and runoff through the solar-radiation data, or to use air temperature associated with different weather patterns. Evaporation and condensation are either mutually compensatory or of negligible effect during other synoptic situations. Spatial distribution of ice-formation zones yielded the upper boundary of liquid runoff at 5200 m.

Accumulation processes were associated with cold cyclonic weather. Estimates of annual accumulation were obtained from 4150–6300 m and increase the amount of information about precipitation distribution in the accumulation areas of the Tien Shan sub-continental glaciers. Spatial distribution of ice-formation zones revealed that the recrystallization zone is above 5800 m. Four ice-formation zones have been revealed in the southern Inylchek glacier accumulation area.

The net glacier mass change is negative, $-318\ \text{g m}^{-2}\ \text{a}^{-1}$, indicating degradation of modern Pobeda–Khan Tengry glaciers.

ACKNOWLEDGEMENTS

This work was supported by the Russian Academy of Science and EOS NASA grant NTW-2602. The authors thank Grant Instruments (Cambridge) Ltd and especially the chairman C. Chapman, director J. Barker and engineer J. Cook, for sponsoring the excellent hydrometeorological Mini-Met stations. We are also very grateful to all the members of our expeditions: A. Dikih, I. Racek, R. Kattelmann, K. Elder, E. Ermolin, G. Kotov and A. Aizen. We thank U. Golodov for his excellent organization of helicopter and provision support.

REFERENCES

Academia Sinica. 1986–87. *[Glacier inventory of China. III. Tien Shan mountains.]* Lanzhou, Lanzhou Institute of Glaciology and Cryopedology. [In Chinese.]

Ahlmann, H.W:son. 1940. The relative influence of precipitation and temperature on glacier regime. *Geogr. Ann.*, **22**(3–4), 188–205.

Aizen, V. B. and E. M. Aizen. 1994a. Features of regime and mass exchange of some glaciers on central Asia periphery. *Bull. Glacier Res.* 12, 9–24.

Aizen, V. B. and E. M. Aizen. 1994b. Regime and mass energy exchange of subtropical latitude glaciers under monsoon climatic conditions: Gongga Shan, Sichuan, China. *Mt. Res. Dev.*, **14**(2), 101–118.

Aizen, V., E. Aizen and J. Melack. 1995. Characteristics of runoff formation at the Kirgizskiy Alatoo, Tien Shan. *International Association of Hydrological Sciences Publication* 228 (Symposium at Boulder 1995 — *Biogeochemistry of Seasonally Snow-Covered Catchments*), 413–430.

Aizen, V., E. Aizen, J. Melack and T. Martma. 1996a. Isotopic measurements of precipitation on central Asia glaciers (southeastern Tibetan, northern Himalayas, central Tien Shan). *J. Geophys. Res.*, **101**(D4), 9185–9196.

Aizen, V. B., E. M. Aizen and J. M. Melack. 1996b. Precipitation, melt and runoff in the northern Tien Shan. *J. Hydrol.*, **186**, 229–251.

Berg, L. S. 1938. *Osnovy klimatologii [The basis of climatology].* Leningrad, Uchebnaya Literatura.

Cheng Tong, *ed.* 1982. *Mount Tuomuer scientific expedition.* Ürümqi, Academia Sinica. Xijiang Peoples Press.

Dolgushin, L. D. and G. B. Osipova. 1980. *Ledniki [Glaciers].* Moscow, Priroda Mira.

Epstein, S. and T. Mayeda. 1953. Variations of O^{18} content of waters from natural sources. *Geochim. Cosmochim. Acta*, **4**(5), 213–224.

Grudzinskiy, M. A. 1959. Lednik Zvezdochka [Zvezdochka glacier]. *In Pobezhdennyye versh'ny [Victory peaks].* Moscow, Geograficheskaya Literatura, 167–214.

Higuchi, K. and Xie Zichu, *eds.* 1989. Glaciological studies in west Kunlun mountains, 1987. *Bull. Glacier Res.* 7.

Kazanskiy, A. B. 1965. O kriticheskom chisle Richardsona [About Richardson's critical number]. *In Fizika atmosferi i okeana [The physics of atmosphere and ocean]. Part I.* Moscow, Akademiya Nauk SSSR, 875–879.

Kobisheva, N.V., *ed.* 1990. *Nauchno-prikladnoy spravochnik po klimatu SSR: Kazakhskaya SSR, Kirgiskaya SSR. Mnogoletniye dannyye [Reference book of climate USSR: Kazakhskaya SSR, Kirgiskaya SSR. Long-term data]. Vol. 18, parts 1, 2, 4; Vol. 32, parts 1, 2, 4.* Leningrad, Gidrometeoizdat.

Konovalov, V. G. 1979. *Raschet i prognoz tayaniya lednikov Sredney Azii [Calculating and forecasting glacier ablation in central Asia].* Leningrad, Gidrometeoizdat.

Krenke, A. N. 1982. *Massoobmen v lednikovykh sistemakh na territorii SSSR [Mass exchange in glacier systems of the U.S.S.R.].* Leningrad, Gidrometeoizdat.

Kurowski, L. 1891. Die Höhe der Schneegrenze mit besonderer Berücksichtigung der Finsteraarhorn-Gruppe. *Geogr. Abh., Berl. Univ.*, **5**(1), 119–160.

Ma Hong, Liu Zongchao and Liu Yifeng. 1992. Energy balance of a snow cover and simulation of snowmelt in the western Tien Shan mountains, China. *Ann. Glaciol.*, **16**, 73–78.

Monin, A. S. and A. M. Obukhov. 1954. Osnovniye kharakteristici turbulentnogo peremeshivaniya v prizemnom sloe atmosferi [Main characteristics of turbulent mixing in atmospheric boundary layer]. *Tr. Inst. Geofiz., Akad. Nauk SSSR*, **24**(151), 3–17.

Racek, V. I. 1954. Oledeneniye massiva pika Pobedi [Glaciation of Peak Pobeda massif]. *Geogr. Sb.*, **4**, 59–81.

Shumskiy, P. A. 1978. *Dynamic glaciology.* New Delhi, Amerind Publishing Co.

Xie Zichu, Zheng Benxing, Li Jijun and Shi Yafeng. 1982. [The distribution, features and variations of glaciers in China.] *In Proceedings of the Symposium on Glaciology and Cryopedology held by the Geographical Society of China, Lanzhou, November 27 – December 3, 1978. Vol. 1.* Beijing, Science Press, 1–13. [In Chinese.]

Yang Zhenniang. 1988. [General situation of research on hydrology of glaciers in China in the last thirty years.] *J. Glaciol. Geocryol.*, **10**(3), 256–261. [In Chinese.]

Zikin, E. M. 1962. *Mass accumulation in firn glacial zones (method of investigation based on temperature profile).* Moscow, AS USSR Publishing. [In Russian.]

MS received 14 March 1996 and accepted in revised form 30 June 1997